

This is an Open Access document downloaded from ORCA, Cardiff University's institutional repository:<https://orca.cardiff.ac.uk/id/eprint/165259/>

This is the author's version of a work that was submitted to / accepted for publication.

Citation for final published version:

Xu, Chen, Jurikova, Hana, Nuber, Sophie, Steele, Robert C. J., Trudgill, Molly, Barker, Stephen, Lear, Caroline H., Burke, Andrea and Rae, James 2024. A rapid, simple, and low-blank pumped ion-exchange column chromatography technique for boron purification from carbonate and seawater matrices. *Geochemistry, Geophysics, Geosystems*

Publishers page: *Geochemistry, Geophysics, Geosystems* <*Geochemistry, Geophysics, Geosystems*>

Please note:

Changes made as a result of publishing processes such as copy-editing, formatting and page numbers may not be reflected in this version. For the definitive version of this publication, please refer to the published source. You are advised to consult the publisher's version if you wish to cite this paper.

This version is being made available in accordance with publisher policies. See <http://orca.cf.ac.uk/policies.html> for usage policies. Copyright and moral rights for publications made available in ORCA are retained by the copyright holders.



1
2 **A rapid, simple, and low-blank pumped ion-exchange column chromatography**
3 **technique for boron purification from carbonate and seawater matrices**

4 **Chen Xu^{1*}, Hana Jurikova¹, Sophie Nuber^{1,2,3}, Robert C.J. Steele¹, Molly Trudgill^{1,4},**
5 **Stephen Barker², Caroline H. Lear², Andrea Burke¹, and James Rae¹**

6 ¹ School of Earth and Environmental Sciences, University of St Andrews, St Andrews, UK.

7 ² School of Earth and Environmental Sciences, Cardiff University, Cardiff, UK.

8 ³ Department of Geosciences, National Taiwan University, Taipei, Taiwan.

9 ⁴ Laboratoire des Sciences du Climat et de l'Environnement, LSCE/IPSL, CEA-CNRS-UVSQ,
10 Université Paris-Saclay, France.

11
12 Corresponding author: Chen Xu (cx23@st-andrews.ac.uk)

13 **Key Points:**

- 14 • A new peristaltic pump-based boron ion-exchange column chromatography, achieving 8-
15 fold faster boron separation.
- 16 • This technique produces lower total procedure boron blanks than gravity columns.

17 **Abstract**

18 Boron isotopes ratios ($\delta^{11}\text{B}$) are used across the Earth Sciences and are increasingly analysed by
19 Multi-Collector Inductively Coupled Plasma Mass Spectrometry (MC-ICPMS). Accurate $\delta^{11}\text{B}$
20 MC-ICPMS analysis requires boron purification from the sample matrix using ion-exchange
21 column chromatography. However, the traditional gravity-drip column method is time-
22 consuming and prone to airborne contamination due to the long duration and open resin surface.
23 To address these issues, we designed a novel, simple and reliable column chromatography
24 technique called “peri-columns”. This method uses a peristaltic pump to generate vacuum on a
25 commonly used column set up. This method uses sealed collection beakers and does not require
26 solutions to pass through pump tubing, minimising contamination. The duration is reduced by
27 eight-fold, processing 12 samples in just 1.5 hours. It also yields low and consistent total
28 procedural blanks (TPBs), averaging 11 pg. The efficiency and efficacy of this method were
29 tested by repeated boron purification from calcium carbonate and high-sodium matrices with
30 international and in-house reference materials (RM). The results matched those obtained with the
31 gravity column method and fell within our laboratory long-term and international certified
32 values. The mean $\delta^{11}\text{B}$ and 2SD (standard deviation) of repeatedly processed NIST 8301f was
33 $14.57 \pm 0.26 \text{ ‰}$ ($n = 31$), NIST 8301c was $24.19 \pm 0.33 \text{ ‰}$ ($n = 10$), STAiG-F1 was 16.20 ± 0.26
34 ‰ ($n = 13$) and seawater was $39.52 \pm 0.32 \text{ ‰}$ ($n = 10$). All the components of our techniques are
35 commercially available, and it is easily adaptable to other laboratories and isotope systems.

36 **Plain Language Summary**

37 Scientists use boron isotope ratios to study changes in seawater acidity, atmospheric carbon
38 dioxide levels, pollution, and volatile cycling in the Earth. To measure these changes, they need

39 to purify boron from a carbonate matrix, such as foraminifera and coral fossils, or seawater,
40 using ion-exchange column chromatography. However, the traditional gravity-drip column
41 method is time-consuming and prone to airborne contamination. To address this issue, we
42 developed a new technique called "peri-columns", where we connect manufactured columns to a
43 peristaltic pump. The pump creates a vacuum, which pulls the liquid through columns faster than
44 gravity. This new method is around eight times faster than the existing gravity method and, due
45 to the shorter timescale and the closed nature of the columns, produces lower levels of
46 contamination. We tested this technique using several international and in-house reference
47 materials and found that it produced the same boron isotope ratios results as the traditional
48 method, but faster and cleaner.

49 **1 Introduction**

50 Boron is significantly fractionated in nature, due to the large mass difference between B
51 isotopes and high geochemical reactivity. This has made it an invaluable tracer of processes
52 ranging from subduction (De Hoog & Savov, 2018; Regier et al., 2023), paleoenvironmental
53 changes in loess–paleosol sequences (Wei et al., 2015), weathering (Ercolani et al., 2019; Muttik
54 et al., 2011), and waste water (Kloppmann et al., 2008). Boron isotopes are also a key tracer in
55 paleoclimate and paleoceanography studies, due to their ability to record oceanic pH and the
56 subsequent determination of oceanic and atmospheric CO₂ (Dai et al., 2022; Foster, 2008;
57 Honisch et al., 2009; Jurikova et al., 2020; Rae et al., 2018; Shankle et al., 2021; Shao et al.,
58 2019).

59 Over the last 15 years, boron isotope measurements have been increasingly analysed by
60 multi-collector inductively coupled plasma mass spectrometry (MC-ICPMS) (Foster, 2008;
61 Foster et al., 2013; Gutjahr et al., 2021; Rae et al., 2018; Stewart et al., 2021). For accurate
62 solution-based MC-ICPMS analysis, boron purification is required to minimise the impact of
63 matrix effects and isobaric interferences from the sample matrix (Chen et al., 2016; Foster et al.,
64 2013; Foster et al., 2018; Gutjahr et al., 2021; Lemarchand et al., 2002; Stewart et al., 2021).

65 Currently, most commonly used methods for boron purification are based on ion
66 exchange, gravity column chromatography (Foster, 2008; Foster et al., 2013; Gutjahr et al.,
67 2021; Stewart et al., 2021), and to a lesser extent microsublimation (Buisson et al., 2021; Misra
68 et al., 2014; Rodríguez-Díaz et al., 2024), batch method (Douville et al., 2010; Lécuyer et al.,
69 2002), and pumped chromatography systems (de la Vega et al., 2020; Wei et al., 2014). The
70 benefit of traditional ion exchange gravity column chromatography techniques lies in the
71 generation of accurate and precise boron isotope data (Gutjahr et al., 2021; Stewart et al., 2021).
72 However, they rely on time-consuming and labour-intensive operation of hand-made gravity
73 columns, with several methodological drawbacks.

74 Firstly, due to the geometry and small size of hand-made microcolumns, drip rates are
75 slow, and so the process of gravity column chromatography is very time-consuming (~6 - 12 hrs
76 for 12 samples, depending on specifics of column performance and lab temperature). Minimising
77 blank contamination and isotopic fractionation is crucial to obtain accurate boron isotope data
78 (Kubota et al., 2021). While blank contributions from labware and reagents can be relatively
79 easily minimised, for B, the major source of contamination during column chromatography
80 might be airborne (Kubota et al., 2021). The purification procedure is normally undertaken in a
81 low-boron clean hood. However, the potential for fall-in blank from the operator's sleeves and/or
82 airborne boron flow into the hood by opening and closing the door, may cause random

83 contamination of the samples during a long operation procedure, which is hard to monitor and
84 mitigate. As such, a shorter operation time should not only increase the lab efficiency but also
85 minimise contamination and isotopic fractionation during the experiment.

86 Secondly, the flow rate of solutions through the traditional gravity columns maybe
87 inconsistent, due to changes in hydrostatic head pressure and variations in geometry column to
88 column. The Microcolumns are typically hand-made from heat shrinking PFA using a heat gun
89 or oven. The manual demoulding process and hand fitting of the frit will inevitably cause some
90 deformation of the neck, shoulders, and other delicate parts of the column, while hand-fitting of
91 the frit may additionally cause closure of the frit pore space, reducing flow rates. These also
92 cause each column to be individually shaped, rather than identical. These geometric differences
93 may lead to inconsistency in the flow rate of solutions between the microcolumns, with the
94 potential to influence the consistency of the matrix separation.

95 Thirdly, the efficient flow of the last reagent droplet through the resin and frit is hindered
96 by the liquid's surface tension when driven by gravity. This issue, known as the “last drop issue”,
97 may result in inaccurate $\delta^{11}\text{B}$ values. Incomplete boron loading or recovery from the Amberlite
98 IRA-743 resin is the leading cause of boron isotope fractionation during the boron purification
99 (Lemarchand et al., 2002). Studies have shown that ^{11}B is more concentrated in the initial elution
100 solution, while ^{10}B is more enriched at the tail (Lemarchand et al., 2002). A 1% loss of the boron
101 at the end of elution can result in a 0.2 ‰ shift in $\delta^{11}\text{B}$ for the recovered solution (Lemarchand
102 et al., 2002). Due to this “last drop issue”, achieving quantitative, complete, and efficient
103 recovery of boron from samples can be challenging. Furthermore, it is crucial to maintain the
104 consistent molarity of nitric acid between sample, standards and blanks in the subsequent MC-
105 ICPMS. Inconsistencies can introduce a matrix effect to the instrument, leading to inaccurately
106 measured $\delta^{11}\text{B}$ values (Chen et al., 2016; Trudgill, 2023). The presence of residual Milli-Q water
107 in the resin after the matrix wash may lead to dilution of the nitric acid concentration for the
108 subsequent boron elution, which can cause such a matrix effect.

109 Efforts have been made to optimise the issues addressed above. A novel design in which
110 the microcolumns are directly connected to a peristaltic pump using peristaltic tubing has been
111 developed (Wei et al., 2014). However, while suitable for some applications, the relatively large
112 procedural blank (TPB) produced from this approach (~0.5 ng), perhaps a function of the direct
113 contact of solutions with pump tubing, would be prohibitive for typical marine carbonate boron
114 isotope sample sizes (~2-20ng). Recently, there have been attempts to optimise the boron
115 purification for coral and seawater samples (de la Vega et al., 2020) using prepFAST Multi
116 Collector (prepFAST) automation system. TPB yield from this method is below 60 pg. However,
117 other marine carbonate matrices with lower boron contents, typical of foraminifera, are yet to be
118 tested.

119 In this study, we developed a highly efficient and low blank peri-column
120 chromatographic system. This system uses a peristaltic pump generated vacuum on
121 commercially available Savillex microcolumns without direct contact with the peristaltic tubing.
122 This method shortens the whole boron purification procedure to 1.5 hours for a batch of 12
123 samples, which enables the integration of sample purification and mass spectrometry in a single
124 day, increasing lab efficiency. This method also shows notable consistency in column
125 performance, due to the equally manufactured column components. Tests on a range of marine
126 carbonate and seawater samples yield data that match literature values for a variety of RMs
127 (Stewart et al., 2021; Trudgill, 2023), and show improved blank contamination control. In

128 addition, this novel method also enables highly efficient preparation of boron-free ammonium
129 acetate buffer for boron purification. The simplicity and accessible nature of this configuration
130 allows its application to a variety of laboratories and isotopic systems and simplifies the
131 protocols for boron purification with a lower blank.

132 **2 Materials and Methods**

133 2.1 Materials

134 2.1.1 Standards and reference materials

135 We used 2ml Savillex Teflon microcolumns with a 5mm diameter capillary packed with
136 20 μ l of crushed and sieved (mesh size 63-150 μ m) Amberlite IRA-743 resin (Kiss, 1988) for
137 boron purification. First, we tested the usability of these columns for boron purification using the
138 standard gravity boron column procedure (see Foster et al., 2008). We then optimised the method
139 and assessed the accuracy and reproducibility of $\delta^{11}\text{B}$ standard values via peri-column. We tested
140 multiple standards and reference materials with varied matrix types and B/Ca ratios including
141 NIST RM 8301 (Coral) (8301c), NIST RM 8301 (Foraminifera) (8301f) (Stewart et al., 2021),
142 in-house mixed and natural foraminifera standard STAiG-F1, and open ocean seawater from
143 Atlantic Ocean, each of which have been thoroughly characterised within the St Andrews Isotope
144 Group (STAiG) (Trudgill, 2023). All sample preparations were undertaken in the STAiG boron-
145 free clean laboratory at the University of St Andrews.

146 2.1.2 Buffer reagent

147 Quantitative absorption of boron from the acid-based sample onto IRA-743 resin can be
148 achieved by raising the pH to 5.5 using a buffer such as ammonium hydroxide, sodium
149 hydroxide, sodium acetate, or ammonium acetate can be added, as demonstrated by Dai et al.,
150 2022; Foster, 2008; Jurikova et al., 2019, and Lemarchand et al., 2002. Marine biogenic
151 carbonate samples, including foraminifera, corals, and brachiopods, are commonly used for
152 boron isotope studies. However, these samples consist mainly of calcite and aragonite, which
153 contain abundant matrix elements such as Ca, Na, and Mg. When the sample is in an alkaline
154 condition, matrix elements can form hydroxide precipitates, which may incorporate boron from
155 the solution, resulting in boron isotopic fractionation (Foster, 2008; Foster et al., 2013;
156 Lemarchand et al., 2002). To prevent the precipitation of hydroxides before loading, the pH of
157 the sample for column loading should be high enough to allow for the binding of boron onto the
158 resin but low enough to avoid the formation of hydroxide precipitates. The buffer reagent used in
159 this study is pre-cleaned boron-free ~ 1.2 M ammonium acetate (de la Vega et al., 2020). This is
160 made from a mixture of 1.4 M ammonium hydroxide and 1.2 M acetic acid. Carbonate samples
161 were dissolved in 0.5 M HNO_3 with an additional 50-100 μ l of ultra-pure water (Milli-Q, 18.2
162 $\text{M}\Omega\cdot\text{cm}$ at 25°C) and then buffered to $\text{pH} \approx 5.5$ with 1.5 times the volume of the 0.5 M HNO_3
163 using pre-cleaned boron-free ~ 1.2 M ammonium acetate. Cleaning of this buffer was also
164 achieved using a peri-column (Table 1).
165

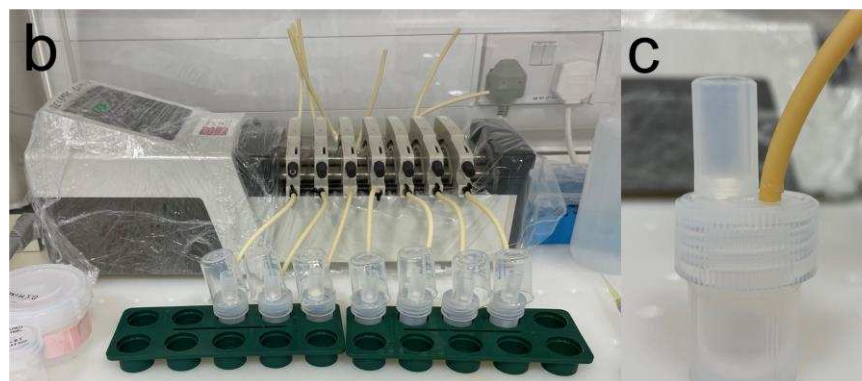
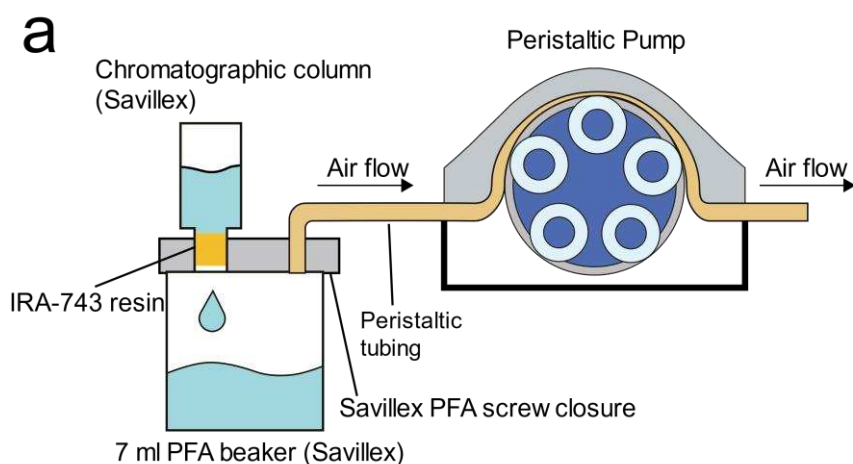
166 **Table 1. Protocols of the preparation for the boron-free $\text{NH}_4\text{CH}_3\text{CO}_2$ buffer using peri-**
167 **column described in this study. Note that a pump speed of 85 RPM corresponds to a flows**
168 **rate of 100 μ l/s.**

Step	Purpose	Reagent	Pump speed (revolutions per minute)	Collection/Discard
1	Resin pre-clean	2 × 2000 μL 0.5M HNO ₃	85	Discard
2	Condition	2 × 2000 μL Milli-Q water	85	Discard
3	Load uncleaned buffer	5 × 2 mL NH ₄ CH ₃ CO ₂ buffer	85	Collect
4	Resin post-clean	2 × 2000 μL 0.5M HNO ₃	85	Discard
5	Condition	2 × 2000 μL Milli-Q water	85	Discard

169

170 2.1.3 Peri-column chromatographic system setup

171 The peri-column system (Figure 1a and b) uses a Watson Marlow 205U/CA auto-control
 172 multi-channel cassette peristaltic pump with 16 tubing positions, Santoprene 2-stop peristaltic
 173 tubing (150 mm bridge, 2.29 mm inner diameter), 2ml Savillex Teflon microcolumns with 20μl
 174 of Amberlite IRA 743 resin, and 7 ml Savillex Teflon vials with openings in the lids drilled using
 175 a drill bit with a diameter of 3.5 mm to fit the peristaltic tubing and a 6.5 mm bit to seat the
 176 column itself (Figure 1c). By pumping out air from the vial headspace, a negative pressure
 177 gradient can be created between the vials and the supernatant solution above the resin bed. This
 178 allows for solutions to pass quickly and steadily through the resin in the columns without coming
 179 into contact with the tubing. To ensure airtightness and consistency of this closed system,
 180 customised 2ml Savillex Teflon microcolumns were used instead of the fragile hand-made
 181 columns.



182

183 **Figure 1. a.** Schematic illustration of the peri-column system. **b.** Photo of our peri-column setup
184 in the clean laboratory at STAiG. **c.** A close-up photo showing a chromatographic column and a
185 peristaltic tubing fitted into the 7ml Savillex Teflon vial.

186 2.1.4 PFA vials and plastics

187 Two pre-cleaned 7ml Savillex Teflon vials per sample are required for collecting the
188 separated boron and an extra elution ‘tail’. To clean the vials, they were firstly filled with 7 M
189 HNO₃ (reagent grade), capped, and left on a hot plate at 140 °C overnight, and then rinsed with
190 Milli-Q water three times. Then, we used KimWipes to wipe the interior of the vials and lid with
191 acetone to remove any organic residues, followed by triple rinsing with Milli-Q water. Next, they
192 were placed in a Teflon jar filled with 7 M HNO₃ (reagent grade), left on a hot plate overnight,
193 and again rinsed with Milli-Q water three times. The process was then repeated with 6 M HCl
194 (reagent grade). One day before the column chromatography, the Teflon vials were filled with
195 1.5 M HNO₃ (distilled grade) and left on a hot plate overnight. They were rinsed with Milli-Q
196 water three times and dried in a boron-free clean hood.

197 Samples were analysed in 2 ml pre-cleaned Eppendorf centrifuge tubes per sample,
198 which fit directly into the CETAC ASX-100 Micro Autosampler. To prepare the centrifuge
199 tubes, we submerged them into a plastic jar filled with 1 M HCl (distilled grade) and placed them
200 on a hot plate at 60 °C overnight. Tubes were then rinsed with Milli-Q water three times and
201 dried in a clean hood. Before the column chromatography, we rinsed the tubes with 1.5 M HNO₃
202 (distilled grade) once and Milli-Q water three times using a wash bottle.

203 The freshly drilled lids of the 7 mL Savillex Teflon vials were first smoothed with
204 sandpaper and intensely rinsed with Milli-Q water until no visible residue remained attached.
205 The surface and holes were then physically cleaned using acetone on a lab wipe. Subsequently,
206 the lids were cleaned following the same procedure as the centrifuge tubes. The used 1 M HCl
207 (distilled grade) solution was discarded. After that, the lids underwent additional cleaning via the
208 aforementioned 7 M HNO₃ (reagent grade) and 6 M HCl (reagent grade) bath procedure that is
209 used for the Teflon vials. They were then rinsed with 1.5 M HNO₃ (distilled grade) applied via
210 wash bottle, followed by triple Milli-Q water rinses.

211 Because the duration of the peri-column procedure is short and drilled lids do not make
212 direct contact with reagents or samples, stringent cleaning between uses, as done for the Teflon
213 vials used to catch eluates, is not essential for lids. After each use with the peri-column, the lids
214 should be wiped with acetone and Milli-Q water and stored in cleaned plastic bag. Before the
215 next usage, the lids were cleaned following the aforementioned centrifuge tube cleaning
216 procedure.

217 2.2 Gravity column chromatography for boron purification

218 The columns were firstly cleaned by multiple rinse of 0.5 M HNO₃ and Milli-Q water to
219 remove any potential residues of boron and matrix elements. Subsequently, the sample-buffer
220 mixtures were slowly pipetted dropwise into the columns to allow the boron within the solution
221 to be better captured by the boron-specific resin and to avoid disturbance of the resin bed. The
222 maximum volume pipetted in during sample loading is 200 µl; any larger sample-buffer volumes
223 were loaded in multiple applications. To wash out the matrix elements, the columns underwent
224 eleven rinses with 150 µl of Milli-Q water. This was followed by carefully pipetting 100 µl of
225 0.5 M HNO₃ through the columns to elute the boron bound to the resin. To ensure complete

226 boron recovery, and sufficient volume for MC-ICPMS analysis, 600 μL of 0.5 M HNO_3 was
 227 used, meaning this step is repeated 6 times. The actual volume of eluant acid can be adjusted
 228 depending on the carbonate sample size, mass spectrometry method, and resin performance
 229 varying across different labs by checking the column calibration. To confirm the complete
 230 recovery of all the boron from the resin, an additional 100 μL of 0.5 M HNO_3 was passed through
 231 the column and collected, known as the "tail".

232 2.3 Operating procedures for the peri-column

233 The overall procedure for the peri-column follows a similar structure to the gravity
 234 approach, including column pre-wash, sample loading, matrix wash, elution, and column re-wash
 235 steps. However, it has been optimised to produce faster and more consistent results. Table 2
 236 provides a detailed protocol. Once the reagent was pipetted into the peri-column, the peristaltic
 237 pump was activated with a pump speed of 85 revolutions per minute (RPM) to accelerate the
 238 flow. It is advised to maintain the pump speed below 85 RPM to prevent frit tilting and the
 239 associated resin leakage. The flow rate of peri-column is approximately 100 $\mu\text{L}/\text{s}$. The peristaltic
 240 pump should not be used to increase the flow rate during sample loading, as rapid flow can lead
 241 to incomplete boron capture by the resin and unwanted fractionation (Section 3.1).

242 To remove matrix elements in the sample, we performed 7 rinses using 500 μL of Milli-Q
 243 water, which is a reduced rinse number compared to gravity column method (11 steps with 150
 244 μL). Following the completion of matrix wash, pre-cleaned 7ml Savillex Teflon vials were
 245 screwed onto the system to collect the eluted samples. A volume of 600 μL 0.5 M HNO_3 is
 246 sufficient to achieve over 99% boron recovery using the peri-column method. Similarly, another
 247 set of pre-cleaned 7ml Savillex Teflon vials was connected to the peri-column to collect the tail
 248 elution. After the tail elution was completed, the Teflon vials used for column wash were
 249 reconnected peri-column to clean and condition the resin for storage.

250 **Table 2. Protocols of the boron separation using the peri-column approach described in**
 251 **this study.**

Step	Purpose	Reagent	Pump speed (RPM)	Collection/Discard
1	Resin pre-clean	2 \times 2000 μL 0.5M HNO_3	85	Discard
2	Condition	2 \times 2000 μL Milli-Q water	85	Discard
3	Load sample	$\text{NH}_4\text{CH}_3\text{CO}_2$ - sample mixture	0	Discard
4	Matrix wash	7 \times 500 μL Milli-Q water	85	Discard
5	Boron elution	5 or 6 \times 100 μL 0.5M HNO_3	85	Collect
6	Tail elution	100 μL 0.5M HNO_3	85	Collect
7	Resin post-clean	2 \times 2000 μL 0.5M HNO_3	85	Discard
8	Condition	2 \times 2000 μL Milli-Q water	85	Discard

252 2.4 Mass spectrometry

253 Purified samples were transferred from 7ml Savillex Teflon vials into pre-cleaned 2 ml
 254 Eppendorf centrifuge tubes prior to analysis. 10 μL splits of each purified sample were extracted
 255 into another batch of 2 ml Eppendorf centrifuge tubes and diluted with 140 μL 0.5 M HNO_3 .
 256 These samples were analysed for concentrations of B ([B]) and Na ([Na]), Mg ([Mg]), and Ca

257 ([Ca]) to assess the effectiveness of matrix wash and boron recovery. This was done before
258 conducting the $\delta^{11}\text{B}$ analysis by peak hopping on the MC-ICPMS.

259 Boron isotope analysis was performed on a Thermo Fisher Neptune Plus MC-ICPMS at
260 STAiG using sample-standard bracketing (Foster, 2008; Foster et al., 2013; Rae et al., 2018; Rae
261 et al., 2011). Prior to analysis, purified samples, blanks, and standards were spiked with
262 concentrated HF to yield a solution of 0.5 M HNO_3 -0.3 M HF. This spiking aimed at minimising
263 boron evaporation, reducing background, facilitating boron wash out, and shortening the
264 bracketing time (Misra et al., 2014; Rae et al., 2018; Zeebe & Rae, 2020). The same batch of
265 distilled 0.5 M HNO_3 was used for sample elution, dilution of the bracketing standard NIST
266 SRM 951, and preparation of instrumental blanks. This ensured accurate background correction
267 via on-peak zeroing and consistent instrumental matrix effects. To monitor the accuracy and
268 consistency of the analytical sequence, multiple measurements of Ca-free boric acid standards
269 ERM-AE121 (Vogl et al., 2010) and BIGD (Foster et al., 2013) were taken and produced
270 identical results. The propagated analytical error for $\delta^{11}\text{B}$ analysis for these 7.5ng boron samples,
271 which yielded 12.5 ppb analytical solutions, was estimated over multiple analyses of 7.5-15ng
272 boron at STAiG. This long term standard deviation (2σ) was $<0.21\text{‰}$ (Trudgill, 2023).

273 The matrix element and boron concentrations during the Milli-Q matrix removal steps
274 were analysed on an Agilent 8900 QQQ-ICP-MS (QQQ) at STAiG, spiking the Milli-Q washes
275 with concentrated HNO_3 to give a solution of 0.5 M HNO_3 . The typical reproducibility for Ca,
276 Mg, Na, Sr, Al, Mn and B was better than 3% 2RSD (relative standard deviation). Note that this
277 trace element analysis was only performed to verify the reliability of the two column methods
278 and is not part of the procedure for routine $\delta^{11}\text{B}$ analysis.

279 2.5 Pump speed test

280 To explore the shortest duration for the total procedure for a reliable peri-column method,
281 we tested the fastest peristaltic pump speed at which reliable $\delta^{11}\text{B}$ values can be produced.
282 Because both incomplete boron capture during sample loading and incomplete boron collection
283 during elution can result in isotopic fractionation, testing accelerated flow rates in both stages is
284 required to verify reproducibility. 90 RPM is the maximum speed for our peristaltic pump. We
285 first tested $\delta^{11}\text{B}$ values of standard 8301f using the peristaltic pump at 90 RPM throughout all
286 column chromatography steps. A second test turned off the pump, during sample loading only,
287 but otherwise maintained 90 RPM.

288 High pump speeds might destabilise the frit in the column, thereby shortening the lifetime
289 of the peri-column system. Observation of the position and flatness of the frit in the column is
290 recommended after each use. If signs of frit instability are observed, the pump speed should be
291 reduced until frit movement ceases. The optimal pump on/off sequence identified previously will
292 then be re-examined to verify the suitability of this new pump speed.

293 3 Results and discussion

294 3.1 Pump speed

295 The total duration of the peri-column method was determined by the speed setting of the
296 peristaltic pump. Our objective was to find the highest pump speed that would produce
297 consistently good results. After testing multiple speeds, we discovered that continuously using
298 the maximum pump speed of 90 RPM caused instability of the frit, leading to resin leakage from

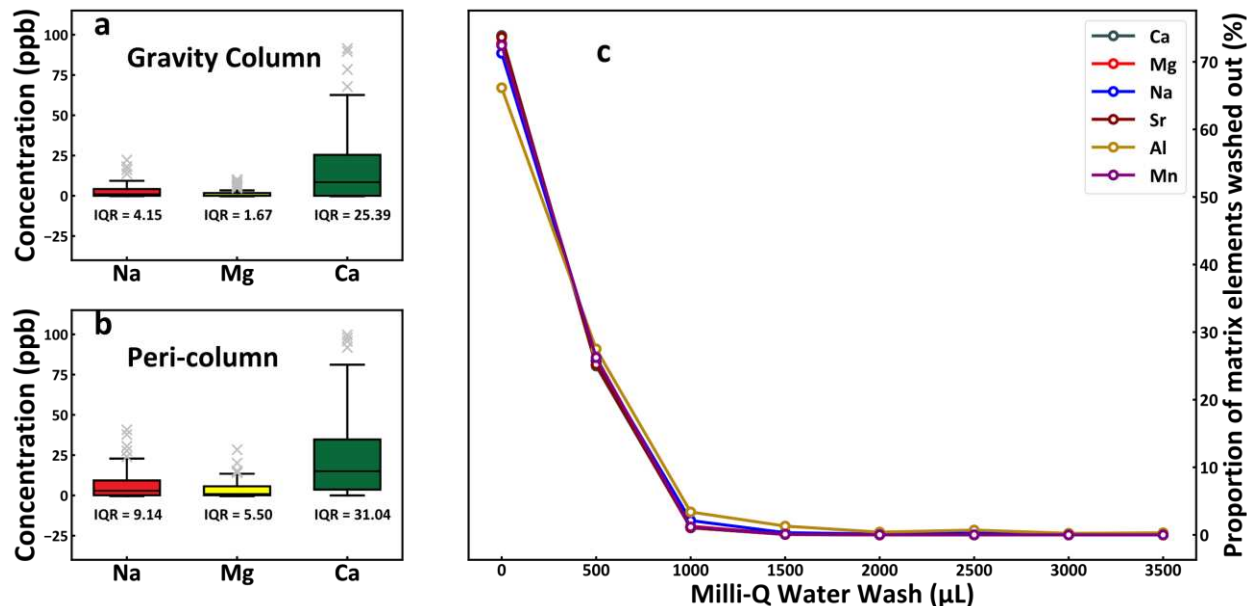
299 the column. We therefore slowed down the peristaltic pump speed to 85 RPM as a compromise
300 between procedural duration and frit stability.

301 Our additional tests show no fractionation for the accelerated elution step. However,
302 using the peristaltic pump during the loading stage of the standard 8301f resulted in low and
303 variable $\delta^{11}\text{B}$ values of 13.86 ± 0.91 ‰ (2 standard deviation (SD), $n = 14$) (Figure 4a), which is
304 significantly offset from the certified values (Stewart et al., 2021) and STAiG long-term mean
305 $\delta^{11}\text{B}$ value (14.61 ± 0.21 ‰, 2SD; between 2019-2023) (Trudgill, 2023). We attribute this to the
306 incomplete boron capture in the resin caused by excessive pump speed during the sample loading
307 stage. This is consistent with variable loss of isotopically-heavy boric acid during loading, with
308 the fast transit speed preventing re-speciation to the borate form that absorbs to the resin
309 (Lemarchand et al., 2002). To combat this, we suggest utilising gravity loading instead of
310 peristaltic pump acceleration during the sample loading stage. At the optimal setting of gravity
311 speed during loading, and 85 RPM during the remainder of the protocol, the purification protocol
312 can be completed in 1.5 hours for 12 samples. This is 4.5-10.5 hours faster than the traditional
313 approach.

314 3.2 Matrix element removal and boron recovery

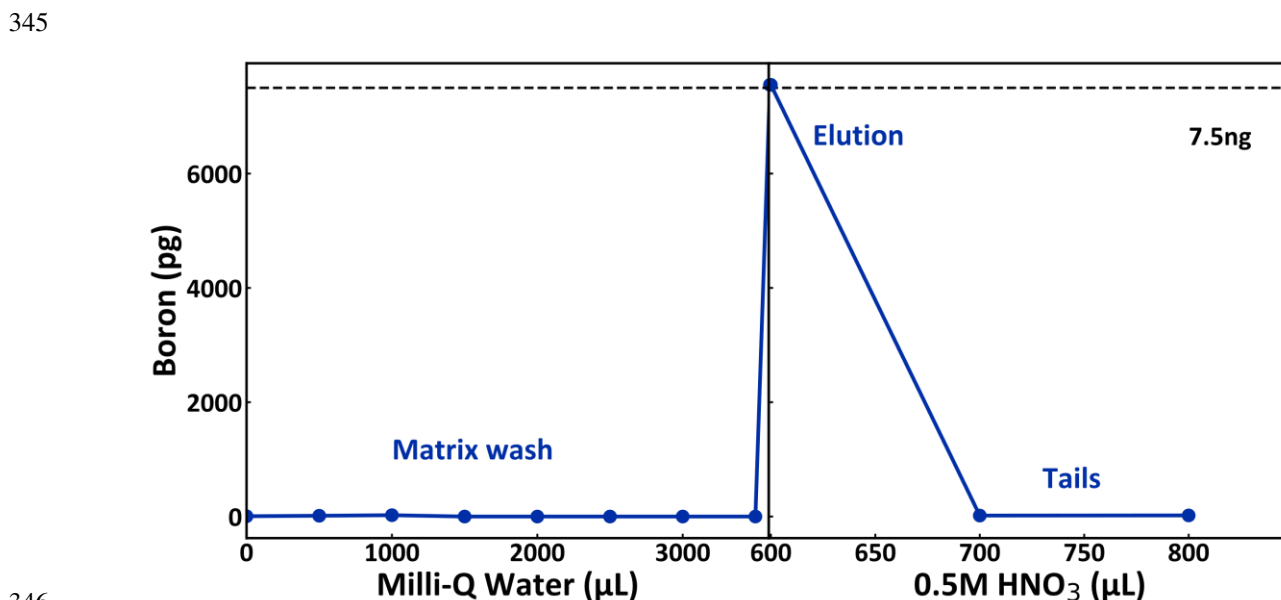
315 Effective removal of matrix elements, such as Mg, Ca, and Na, is crucial in boron column
316 chemistry to prevent impact of matrix effects and isobaric interferences in subsequent analysis
317 on the MC-ICPMS (Foster et al., 2013; Foster et al., 2018; Gutjahr et al., 2021; Stewart et al.,
318 2021). Therefore, any purification method aimed at analysing $\delta^{11}\text{B}$ must demonstrate effective
319 removal of other matrix elements. Here we conduct a step-by-step examination of matrix
320 elements in the wash with 8301f, using an aliquot with 7.5 ng B, 200 μg Ca, 318 ng Mg, and 351
321 ng Na. A persistent decrease in the concentration of each matrix element through each Milli-Q
322 rinse is clearly observed (Figure 2c). Key matrix elements from the artificial foraminiferal
323 CaCO_3 standard (e.g. Ca, Sr) fall to values indistinguishable from the instrumental background.
324 Other elements including Mg, Na, Al and Mn stay slightly above background at the final wash
325 but are lower than 1 ppb.

326 We evaluated the efficacy of matrix element removal for both the standard gravity
327 method and the peri-column approach by analysing the [Na], [Mg], and [Ca] in the purified
328 samples. We use reference materials 8301c, 8301f, and STAiG-F1 with 7.5 ng of boron in each
329 loaded aliquot. Throughout our analyses, the concentrations of [Na], [Mg], and [Ca] in the
330 purified samples were all below 0.1% of the amount loaded onto columns (Figure 2a and b). This
331 indicates that both methods demonstrated similar and effective matrix element removal,
332 consistent with the literature (Chen et al., 2016; de la Vega et al., 2020; Foster, 2008; Guerrot et
333 al., 2011).



334
 335 **Figure 2.** Box and whisker plot for the concentrations of matrix elements Na, Mg, and Ca in the
 336 aliquot of the final sample by gravity approach (a) and peri-column approach (b). Interquartile
 337 Ranges (IQR) are indicated below each boxplot. Outliers are grey cross markers. c. Proportions of
 338 matrix elements washed out from each Milli-Q water rinse step using peri-column.

339 Accurate $\delta^{11}\text{B}$ analysis requires complete boron collection to prevent isotopic
 340 fractionation. [B] evolution curves for the peri-column approach indicates good boron recovery
 341 for 8301f with a 7.5 ng boron sample size (Figure 3). Boron in the most of wash steps was
 342 indistinguishable from background, so there is no major boron loss in the wash steps. Subsequent
 343 tails after 600 μL of 0.5 M HNO_3 elution contained less than 20 pg boron (<0.3% of the sample)
 344 (Figure 3), indicating complete elution of boron from the resin during the previous elution steps.



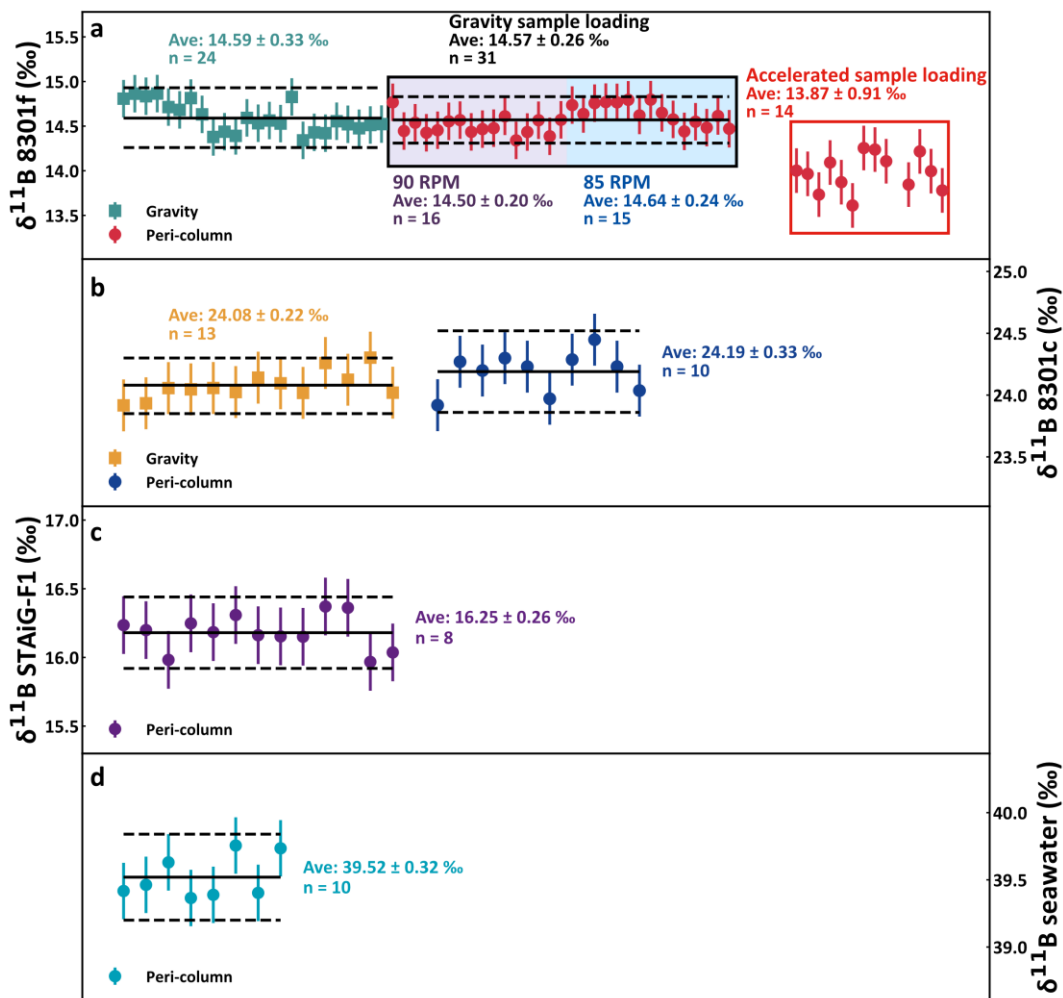
346
 347 **Figure 3.** Boron evolution curve through matrix wash and elution from a 15ppb 8301f standard
 348 (7.5ng boron). The dashed line indicates 7.5 ng boron, the loaded mass.

349 3.3 Reproducibly and accuracy of $\delta^{11}\text{B}$ values from the peri-column chromatography

350 The mean $\delta^{11}\text{B}$ and 2SD for peri-column analyses of standards was $14.57 \pm 0.26 \text{ ‰}$
 351 (2SD) ($n = 31$) for 8301f, $24.19 \pm 0.33 \text{ ‰}$ (2SD) ($n = 10$) for 8301c, $16.20 \pm 0.26 \text{ ‰}$ (2SD) ($n =$
 352 13) for STAiG-F1, and $39.52 \pm 0.32 \text{ ‰}$ (2SD) ($n = 10$) for seawater (Figure 4). These results
 353 align with those generated using traditional gravity method with the same set of columns (Figure
 354 4a and b) and fall within the range of the respective certified values (Stewart et al., 2021;
 355 Trudgill, 2023). Cross plots of $\delta^{11}\text{B}_{8301f}$ and $\delta^{11}\text{B}_{8301c}$ produced by the same Saville columns via
 356 the traditional gravity method and peri-column approach show a negligible offset $0.06 \pm 0.32 \text{ ‰}$
 357 (2SD) ($n = 10$) for 8301f and $-0.09 \pm 0.19 \text{ ‰}$ (2SD) ($n = 5$) for 8301c (Figure 5a and b).

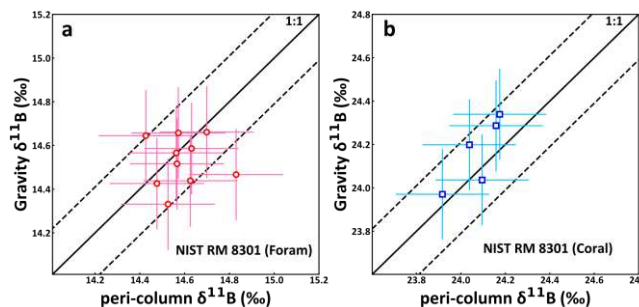
358 We note the hint of some subtle correlation, which may suggest minor systematic
 359 differences between columns, perhaps due to subtleties in frit positioning and geometry that
 360 influence the flow path through the resin or due to the resin itself, but any such effect is small.
 361 All in all, the evidence reviewed here supports that the peri-column method produces accurate
 362 and reproducible $\delta^{11}\text{B}$ data for foraminifera, coral, and seawater matrices, with no significant
 363 fractionation introduced.

364



365 **Figure 4.** $\delta^{11}\text{B}$ values for 7.5 ng boron from reference materials 8301f (a), 8301c (b), STAiG-F1
 366 (c), and seawater (d) processed on gravity columns and peri-columns. Solid line shows the
 367 average value and dashed line shows the 2SD. For panel a, results for 8301f by standard peri-
 368

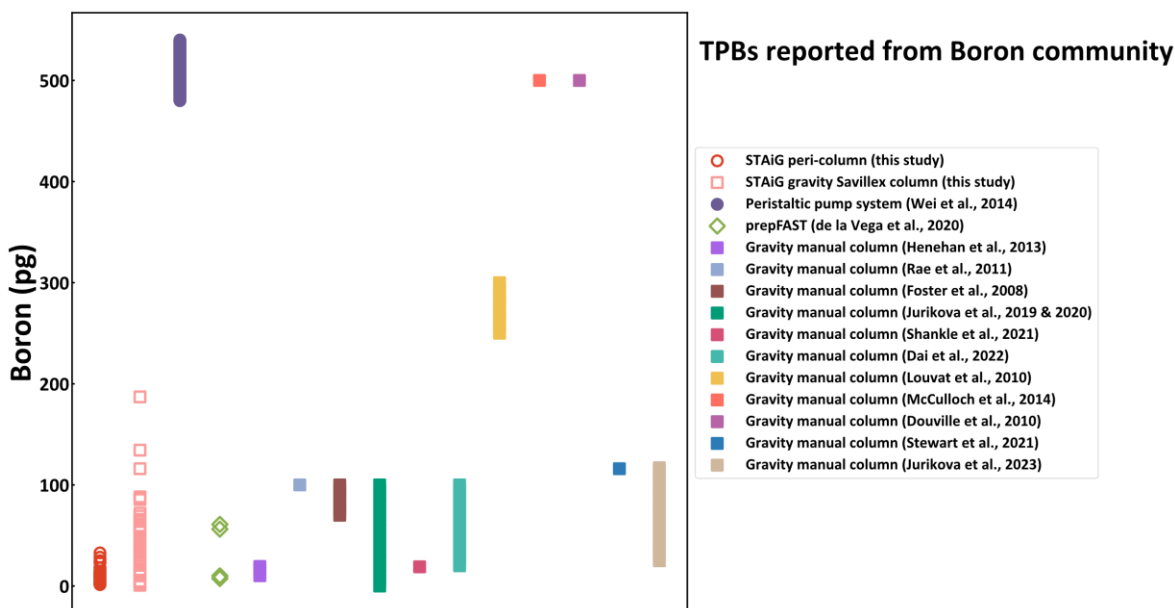
369 column approach are framed in black and shaded in violet and blue respectively for pump speed
 370 with 90 rpm and 85 rpm. The results for undertaking accelerated sample loading are framed in
 371 red.



372
 373 **Figure 5 a, b.** Cross-plots of $\delta^{11}\text{B}$ of 8301f and 8301c prepared by the same column but different
 374 boron separation approaches (traditional gravity method versus this peri-column method). 1:1
 375 ratio line is shown by the solid line and long-term analytical reproducibility (0.21 ‰, 2 σ) is
 376 shown by the dashed lines.

377 **3.4. Total procedural blanks**

378 We assessed TPBs for both protocols by examining Milli-Q Water, 0.5 M HNO₃, and 1.2
 379 M NH₄CH₃CO₂ mixture with the same volume as our samples, through both the traditional
 380 gravity column and peri-column (Figure 6). TPBs obtained from the gravity method is 44 ± 70
 381 pg of boron (n = 52). These values were comparable to the reported TPBs using the gravity
 382 column method by other research groups in the boron community (Dai et al., 2022; de la Vega et
 383 al., 2020; Douville et al., 2010; Foster, 2008; Henehan et al., 2013; Jurikova et al., 2020;
 384 Jurikova et al., 2019; Jurikova et al., 2023; Louvat et al., 2011; McCulloch et al., 2014; Rae et
 385 al., 2011; Shankle et al., 2021; Stewart et al., 2021) (Figure 6). In contrast, the peri-column
 386 yields TPBs of 11 ± 16 pg of boron (n = 33), which are less variable and smaller in size. These
 387 results are similar to those reported by de la Vega (2020) using prepFAST-MC (de la Vega et al.,
 388 2020) and substantially smaller than the previously designed peri-column method where
 389 solutions are in contact with the peristaltic pump tubing (Wei et al., 2014).



391 **Figure 6.** TPBs from peri-column (this study) in comparison to TPBs obtained from the newly
392 published automatic prepFAST method at University of Southampton (de la Vega et al., 2020),
393 old peristaltic pump system approach at Nanjing University (Wei et al., 2014), as well as the
394 traditional gravity column method at University of St Andrews (this study), University of
395 Southampton (Henehan et al., 2013), University of Bristol (Foster, 2008; Rae et al., 2011),
396 GEOMAR (Jurikova et al., 2020; Jurikova et al., 2019), Yale University (Shankle et al., 2021),
397 The Australian National University (Dai et al., 2022), Université Paris-Diderot (Louvat et al.,
398 2011), The University of Western Australia (McCulloch et al., 2014), LSCE/IPSL (Douville et
399 al., 2010), National Institute of Standards and Technology (Stewart et al., 2021), and GFZ –
400 Helmholtz Centre Potsdam (Jurikova et al., 2023).

401 3.5 $\text{NH}_4\text{CH}_3\text{CO}_2$ buffer cleaning by peri-column

402 The cleanliness of peri-column cleaned $\text{NH}_4\text{CH}_3\text{CO}_2$ buffer was assessed by measuring
403 the boron amount in TPBs and evaluating the accuracy of $\delta^{11}\text{B}$ for 8301f produced with buffers
404 of different levels of cleanliness. The loadings for TPBs consisted of 50 μl of Milli-Q, 100 μl of
405 0.5 M HNO_3 plus 150 μl of ~ 1.2 M ammonium acetate buffer. The resulting boron concentration
406 of TPBs produced using uncleaned buffer, peri-column cleaned buffer, and peri-column double
407 cleaned buffer were 6.5, 5.4 and 4.0 pg of boron, respectively. The $\delta^{11}\text{B}$ values for 8301f
408 generated from the aforementioned buffers were 14.71, 14.71, and 14.52, respectively, within \pm
409 0.21 ‰ analytical error of the long-term lab mean (Trudgill, 2023).

410 These results show that the peri-column method effectively produces ammonium acetate
411 buffer of desirable cleanliness levels. Note that the boron concentration of our unclean buffer is
412 already minimal. Nonetheless, we still strongly recommend using cleaned buffer only, as
413 cleanliness may vary between reagent batches and labs. Our method significantly enhances lab
414 efficiency by producing 10 ml of cleaned buffer with a single column in just 10 minutes (Table
415 1).

416 3.6 Molarity effect

417 The use of the peri-column method for boron separation helps minimise the molarity
418 effect on mass spectrometry. To ensure the most accurate $\delta^{11}\text{B}$ analysis on MC-ICPMS, it is
419 crucial to use the same nitric acid used for sample elution for the standards and blanks in the
420 analytical sequence. It has been observed that changing the molarity of nitric acid can introduce a
421 strong matrix effect to the measured $\delta^{11}\text{B}$ values (Chen et al., 2016), especially for small sample
422 sizes (Trudgill, 2023). For the column method, it is difficult for gravity to force the last elution
423 droplet to flow quickly and efficiently through the resin and frit due to the liquid tension. This is
424 called the “last drop issue”. Therefore, the residue of Milli-Q water in the resin after the matrix
425 wash may dilute the concentration of nitric acid for boron elution, resulting in a matrix effect on
426 MC-ICPMS. The liquid within peri-columns is driven by a pressure gradient, resulting in a faster
427 and more complete flow compared to gravity column. No “last drop issue” was observed for
428 peri-columns in this study.

429 3.7 Consistency and lab adaption

430 The consistency of peri-column performance is optimised by employing manufactured
431 Saville microcolumns. With their thick Teflon wall (~ 1 mm), these sturdy columns maintain a
432 consistent shape, including during the frit placement. Drain times for 1.5 ml volumes under

433 gravity alone take 6-10 minutes per column with Savillex microcolumns. This is faster and less
 434 variable than equivalent hand-made columns. Any remaining variability is not attribute to the
 435 geometry of the Savillex column but inconsistencies in frit preparation and placement by hand.

436 In addition, Savillex microcolumns are securely fit into the Teflon vial screw caps and
 437 vacuumed by the high-speed peristaltic pump. When vacuumed at pump speed of 85 RPM, the
 438 columns drain 1.5 ml loads within 15 seconds. The strong and consistent pressure gradient from
 439 the pump normalises any variations between the columns and related setup, for instance, lid
 440 drilling, tubing connections, etc. Nonetheless, caution is advised when setting up this method and
 441 we recommend users check the maximum flow speed for their overall set up or with notably
 442 different column designs.

443 The accessibility of this store-based setup should expand the application of this technique
 444 to other laboratories by reducing the expertise and training required to make and operate
 445 columns.

446 Further studies exploring the application of our peri-column method to other isotope
 447 systems involving chromatographic column purification would be of great interest. Our method
 448 is easily adaptable to other chromatographic procedures and labs given its flexibility, low cost,
 449 cleanliness, and ease of operation. As solutions do not pass through the peristaltic tubing, this
 450 method allows for the use of more concentrated acids, which are commonly used in other
 451 procedures, without the risk of leaching any potential contamination to the samples or damaging
 452 the pump tubing.

453 **4 Conclusions**

454 Our new peri-column boron purification technique enables fast, reliable, and accurate
 455 boron purification for MC-ICPMS. The $\delta^{11}\text{B}$ of foraminifera, coral, and seawater reference
 456 materials match published values and our tests confirm efficient matrix element removal and
 457 complete boron recovery. 12 samples can be processed by this method in 1.5 hours, an 8-fold
 458 reduction compared to traditional gravity columns. Due to the closed nature of this setup and the
 459 shorter air exposure time, the TPB contamination during the boron purification was
 460 consecutively reduced to ~10 pg of boron, substantially lower and more reproducible than typical
 461 gravity column protocols. Additionally, using this peri-column system can efficiently produce
 462 boron-free ammonium acetate buffer, an essential reagent for boron column chromatography.
 463 The simplicity and automation of this setup can be used by a variety of laboratories, simplifies
 464 the purification of boron, and boosts lab efficiency, and would be easily applicable to other
 465 isotopic systems.

466 **Acknowledgments**

467 We thank Heidi Block and Matthew Dumont for analytical and laboratory support. We
 468 also thank Gary Hemming and Troy Rasbury for their encouragement to explore the peristaltic
 469 pump approach. Furthermore, we sincerely thank the careful and detailed assessment by William
 470 Gray and the other anonymous reviewer, which strengthened this manuscript. **Funding:** This
 471 work is supported by the European Research Council under the European Union's Horizon 2020
 472 research and innovation program (grant agreement 805246) to J.W.B.R., H.J., a Natural
 473 Environmental Research Council (NERC)-IAPETUS2 Doctoral Training Programme (DTP)
 474 Studentship to NE/S007431/1 C.X., a NERC-IAPETUS DTP Studentship NE/RO12253/1 to

475 M.T., a Leverhulme Trust Early Career Fellowship ECF-2023-199 to H.J., a NERC UK IODP
 476 grant NE/P000878/1 to S.B. and S.N., and a Taiwanese MOST grant 111-2116M-002-032-MY3
 477 to S.N. **Author contributions:** J.W.B.R., C.X., H.J., S.N., R.S., and A.B. designed the project.
 478 C.X. carried out the column chromatography, trace element concentration analysis. C.X. and H.J.
 479 processed $\delta^{11}\text{B}$ analysis. M.T. contributed to analytics. S.N., C.L., and S.B. provided the
 480 peristaltic pump for this study. C.X. wrote the first draft of manuscript, did the literature data
 481 compilation and figure preparation. All authors read and contributed to the manuscript text. **Data**
 482 **availability:** All data from this study is published in the tables within this manuscript.
 483 **Competing interests:** The authors declare no competing interests.

484 **Open Research**

485 Data Availability Statement: Data generated in this study is included in the manuscript. A link to
 486 the St Andrews Research Repository where the complete dataset will be available when this
 487 manuscript is accepted.

488 **References**

- 489 Buisson, M., Louvat, P., Thaler, C., & Rollion-Bard, C. (2021). High precision MC-ICP-MS
 490 measurements of $^{11}\text{B}/^{10}\text{B}$ ratios from ng amounts of boron in carbonate samples using
 491 microsublimation and direct injection (μ -dDIHEN). *Journal of Analytical Atomic*
 492 *Spectrometry*, 36(10), 2116-2131. <https://doi.org/10.1039/D1JA00109D>
- 493 Chen, X., Zhang, L., Wei, G., & Ma, J. (2016). Matrix effects and mass bias caused by inorganic
 494 acids on boron isotope determination by multi-collector ICP-MS. *Journal of Analytical*
 495 *Atomic Spectrometry*, 31(12), 2410-2417. <https://doi.org/10.1039/C6JA00328A>
- 496 Dai, Y., Yu, J., Ren, H., & Ji, X. (2022). Deglacial Subantarctic CO_2 outgassing driven by a
 497 weakened solubility pump. *Nature Communications*, 13(1), 5193.
 498 <https://doi.org/10.1038/s41467-022-32895-9>
- 499 De Hoog, J. C. M., & Savov, I. P. (2018). Boron Isotopes as a Tracer of Subduction Zone
 500 Processes. In H. Marschall & G. Foster (Eds.), *Boron Isotopes: The Fifth Element* (pp.
 501 217-247). Springer International Publishing. [https://doi.org/10.1007/978-3-319-64666-](https://doi.org/10.1007/978-3-319-64666-4_9)
 502 [4_9](https://doi.org/10.1007/978-3-319-64666-4_9)
- 503 de la Vega, E., Foster, G. L., Martínez-Botí, M. A., Anagnostou, E., Field, M. P., Kim, M. H.,
 504 Watson, P., & Wilson, P. A. (2020). Automation of boron chromatographic purification
 505 for $\delta^{11}\text{B}$ analysis of coral aragonite. *Rapid Communications in Mass Spectrometry*,
 506 34(11), e8762. <https://doi.org/10.1002/rcm.8762>
- 507 Douville, E., Paterne, M., Cabioch, G., Louvat, P., Gaillardet, J., Juillet-Leclerc, A., & Ayliffe,
 508 L. (2010). Abrupt sea surface pH change at the end of the Younger Dryas in the central
 509 sub-equatorial Pacific inferred from boron isotope abundance in corals (*Porites*).
 510 *Biogeosciences*, 7(8), 2445-2459. <https://doi.org/10.5194/bg-7-2445-2010>
- 511 Ercolani, C., Lemarchand, D., & Dosseto, A. (2019). Insights on catchment-wide weathering
 512 regimes from boron isotopes in riverine material. *Geochimica et Cosmochimica Acta*,
 513 261, 35-55. <https://doi.org/10.1016/j.gca.2019.07.002>
- 514 Foster, G. L. (2008). Seawater pH, pCO_2 and $[\text{CO}_3^{2-}]$ variations in the Caribbean Sea over the
 515 last 130 kyr: A boron isotope and B/Ca study of planktic foraminifera. *Earth and*
 516 *Planetary Science Letters*, 271(1), 254-266. <https://doi.org/10.1016/j.epsl.2008.04.015>
- 517 Foster, G. L., Hönisch, B., Paris, G., Dwyer, G. S., Rae, J. W., Elliott, T., Gaillardet, J.,
 518 Hemming, N. G., Louvat, P., & Vengosh, A. (2013). Interlaboratory comparison of boron

- 519 isotope analyses of boric acid, seawater and marine CaCO₃ by MC-ICPMS and NTIMS.
 520 *Chemical Geology*, 358, 1-14. <https://doi.org/10.1016/j.chemgeo.2013.08.027>
- 521 Foster, G. L., Marschall, H. R., & Palmer, M. R. (2018). Boron Isotope Analysis of Geological
 522 Materials. In H. Marschall & G. Foster (Eds.), *Boron Isotopes: The Fifth Element* (pp.
 523 13-31). Springer International Publishing. https://doi.org/10.1007/978-3-319-64666-4_2
- 524 Guerrot, C., Millot, R., Robert, M., & Négrel, P. (2011). Accurate and High-Precision
 525 Determination of Boron Isotopic Ratios at Low Concentration by MC-ICP-MS
 526 (Neptune). *Geostandards and Geoanalytical Research*, 35(2), 275-284.
 527 <https://doi.org/10.1111/j.1751-908X.2010.00073.x>
- 528 Gutjahr, M., Bordier, L., Douville, E., Farmer, J., Foster, G. L., Hathorne, E. C., Hönisch, B.,
 529 Lemarchand, D., Louvat, P., McCulloch, M., Noireaux, J., Pallavicini, N., Rae, J. W. B.,
 530 Rodushkin, I., Roux, P., Stewart, J. A., Thil, F., & You, C.-F. (2021). Sub-Permil
 531 Interlaboratory Consistency for Solution-Based Boron Isotope Analyses on Marine
 532 Carbonates. *Geostandards and Geoanalytical Research*, 45(1), 59-75.
 533 <https://doi.org/10.1111/ggr.12364>
- 534 Henehan, M. J., Rae, J. W., Foster, G. L., Erez, J., Prentice, K. C., Kucera, M., Bostock, H. C.,
 535 Martínez-Botí, M. A., Milton, J. A., & Wilson, P. A. (2013). Calibration of the boron
 536 isotope proxy in the planktonic foraminifera *Globigerinoides ruber* for use in palaeo-CO₂
 537 reconstruction. *Earth and Planetary Science Letters*, 364, 111-122.
 538 <https://doi.org/10.1016/j.epsl.2012.12.029>
- 539 Honisch, B., Hemming, N. G., Archer, D., Siddall, M., & McManus, J. F. (2009). Atmospheric
 540 Carbon Dioxide Concentration Across the Mid-Pleistocene Transition. *Science*,
 541 324(5934), 1551-1554. <https://doi.org/10.1126/science.1171477>
- 542 Jurikova, H., Gutjahr, M., Wallmann, K., Flögel, S., Liebetrau, V., Posenato, R., Angiolini, L.,
 543 Garbelli, C., Brand, U., Wiedenbeck, M., & Eisenhauer, A. (2020). Permian–Triassic
 544 mass extinction pulses driven by major marine carbon cycle perturbations. *Nature*
 545 *Geoscience*, 13(11), 745-750. <https://doi.org/10.1038/s41561-020-00646-4>
- 546 Jurikova, H., Liebetrau, V., Gutjahr, M., Rollion-Bard, C., Hu, M. Y., Krause, S., Henkel, D.,
 547 Hiebenthal, C., Schmidt, M., Laudien, J., & Eisenhauer, A. (2019). Boron isotope
 548 systematics of cultured brachiopods: Response to acidification, vital effects and
 549 implications for palaeo-pH reconstruction. *Geochimica et Cosmochimica Acta*, 248, 370-
 550 386. <https://doi.org/10.1016/j.gca.2019.01.015>
- 551 Jurikova, H., Ring, S. J., Henehan, M. J., Neugebauer, I., Schröder, B., Müller, D., Schwab, M.
 552 J., Tjallingii, R., Brauer, A., & Blanchet, C. (2023). Boron geochemistry reveals the
 553 evolution of Dead Sea brines. *Earth and Planetary Science Letters*, 622, 118403.
 554 <https://doi.org/10.1016/j.epsl.2023.118403>
- 555 Kiss, E. (1988). Ion-exchange separation and spectrophotometric determination of boron in
 556 geological materials. *Analytica Chimica Acta*, 211, 243-256.
 557 [https://doi.org/10.1016/S0003-2670\(00\)83684-3](https://doi.org/10.1016/S0003-2670(00)83684-3)
- 558 Kloppmann, W., Van Houtte, E., Picot, G., Vandenbohede, A., Lebbe, L., Guerrot, C., Millot, R.,
 559 Gaus, I., & Wintgens, T. (2008). Monitoring Reverse Osmosis Treated Wastewater
 560 Recharge into a Coastal Aquifer by Environmental Isotopes (B, Li, O, H). *Environmental*
 561 *Science & Technology*, 42(23), 8759-8765. <https://doi.org/10.1021/es8011222>
- 562 Kubota, K., Ishikawa, T., Nagaishi, K., Kawai, T., Sagawa, T., Ikehara, M., Yokoyama, Y., &
 563 Yamazaki, T. (2021). Comprehensive analysis of laboratory boron contamination for

- 564 boron isotope analyses of small carbonate samples. *Chemical Geology*, 576, 120280.
 565 <https://doi.org/10.1016/j.chemgeo.2021.120280>
- 566 Lécuyer, C., Grandjean, P., Reynard, B., Albarède, F., & Telouk, P. (2002). $^{11}\text{B}/^{10}\text{B}$ analysis of
 567 geological materials by ICP–MS Plasma 54: Application to the boron fractionation
 568 between brachiopod calcite and seawater. *Chemical Geology*, 186(1), 45-55.
 569 [https://doi.org/10.1016/S0009-2541\(01\)00425-9](https://doi.org/10.1016/S0009-2541(01)00425-9)
- 570 Lemarchand, D., Gaillardet, J., Göpel, C., & Manhès, G. (2002). An optimized procedure for
 571 boron separation and mass spectrometry analysis for river samples. *Chemical Geology*,
 572 182(2), 323-334. [https://doi.org/10.1016/S0009-2541\(01\)00329-1](https://doi.org/10.1016/S0009-2541(01)00329-1)
- 573 Louvat, P., Bouchez, J., & Paris, G. (2011). MC-ICP-MS Isotope Measurements with Direct
 574 Injection Nebulisation (d-DIHEN): Optimisation and Application to Boron in Seawater
 575 and Carbonate Samples. *Geostandards and Geoanalytical Research*, 35(1), 75-88.
 576 <https://doi.org/10.1111/j.1751-908X.2010.00057.x>
- 577 McCulloch, M. T., Holcomb, M., Rankenburg, K., & Trotter, J. A. (2014). Rapid, high-precision
 578 measurements of boron isotopic compositions in marine carbonates. *Rapid*
 579 *Communications in Mass Spectrometry*, 28(24), 2704-2712.
 580 <https://doi.org/10.1002/rcm.7065>
- 581 Misra, S., Owen, R., Kerr, J., Greaves, M., & Elderfield, H. (2014). Determination of $\delta^{11}\text{B}$ by
 582 HR-ICP-MS from mass limited samples: Application to natural carbonates and water
 583 samples. *Geochimica et Cosmochimica Acta*, 140, 531-552.
 584 <https://doi.org/10.1016/j.gca.2014.05.047>
- 585 Muttik, N., Kirsimäe, K., Newsom, H. E., & Williams, L. B. (2011). Boron isotope composition
 586 of secondary smectite in suevites at the Ries crater, Germany: Boron fractionation in
 587 weathering and hydrothermal processes. *Earth and Planetary Science Letters*, 310(3),
 588 244-251. <https://doi.org/10.1016/j.epsl.2011.08.028>
- 589 Rae, J. W. B., Burke, A., Robinson, L. F., Adkins, J. F., Chen, T., Cole, C., Greenop, R., Li, T.,
 590 Littley, E. F. M., Nita, D. C., Stewart, J. A., & Taylor, B. J. (2018). CO₂ storage and
 591 release in the deep Southern Ocean on millennial to centennial timescales. *Nature*,
 592 562(7728), 569-573. <https://doi.org/10.1038/s41586-018-0614-0>
- 593 Rae, J. W. B., Foster, G. L., Schmidt, D. N., & Elliott, T. (2011). Boron isotopes and B/Ca in
 594 benthic foraminifera: Proxies for the deep ocean carbonate system. *Earth and Planetary*
 595 *Science Letters*, 302(3-4), 403-413. <https://doi.org/10.1016/j.epsl.2010.12.034>
- 596 Regier, M. E., Smit, K. V., Chalk, T. B., Stachel, T., Stern, R. A., Smith, E. M., Foster, G. L.,
 597 Bussweiler, Y., DeBuhr, C., Burnham, A. D., Harris, J. W., & Pearson, D. G. (2023).
 598 Boron isotopes in blue diamond record seawater-derived fluids in the lower mantle. *Earth*
 599 *and Planetary Science Letters*, 602, 117923. <https://doi.org/10.1016/j.epsl.2022.117923>
- 600 Rodríguez-Díaz, C. N., Paredes, E., Pena, L. D., Cacho, I., Pelejero, C., & Calvo, E. (2024).
 601 Nanogram-scale boron isotope analysis through micro-distillation and Nu Plasma 3 MC-
 602 ICP-MS. *Talanta*, 269, 125473. <https://doi.org/10.1016/j.talanta.2023.125473>
- 603 Shankle, M. G., Burls, N. J., Fedorov, A. V., Thomas, M. D., Liu, W., Penman, D. E., Ford, H.
 604 L., Jacobs, P. H., Planavsky, N. J., & Hull, P. M. (2021). Pliocene decoupling of
 605 equatorial Pacific temperature and pH gradients. *Nature*, 598(7881), 457-461.
 606 <https://doi.org/10.1038/s41586-021-03884-7>
- 607 Shao, J., Stott, L. D., Gray, W. R., Greenop, R., Pecher, I., Neil, H. L., Coffin, R. B., Davy, B., &
 608 Rae, J. W. (2019). Atmosphere-ocean CO₂ exchange across the last deglaciation from the

- 609 Boron Isotope Proxy. *Paleoceanography and Paleoclimatology*, 34(10), 1650-1670.
610 <https://doi.org/10.1029/2018PA003498>
- 611 Stewart, J. A., Christopher, S. J., Kucklick, J. R., Bordier, L., Chalk, T. B., Dapoigny, A.,
612 Douville, E., Foster, G. L., Gray, W. R., Greenop, R., Gutjahr, M., Hemsing, F.,
613 Henehan, M. J., Holdship, P., Hsieh, Y.-T., Kolevica, A., Lin, Y.-P., Mawbey, E. M.,
614 Rae, J. W. B., . . . Day, R. D. (2021). NIST RM 8301 Boron Isotopes in Marine
615 Carbonate (Simulated Coral and Foraminifera Solutions): Inter-laboratory $\delta^{11}\text{B}$ and
616 Trace Element Ratio Value Assignment. *Geostandards and Geoanalytical Research*,
617 45(1), 77-96. <https://doi.org/10.1111/ggr.12363>
- 618 Trudgill, M. D. (2023). *Boron based geochemical reconstructions of ocean pH and atmospheric*
619 *CO₂ in the geological record* [Doctoral thesis, The University of St Andrews].
620 <http://hdl.handle.net/10023/27101>
- 621 Vogl, J., Becker, D., Koenig, M., & Rosner, M. (2010). *Certification report for the reference*
622 *materials ERM-AE102a, -AE104a, -AE120, -AE121 and -AE122*. [https://nbn-](https://nbn-resolving.org/urn:nbn:de:kobv:b43-355813)
623 [resolving.org/urn:nbn:de:kobv:b43-355813](https://nbn-resolving.org/urn:nbn:de:kobv:b43-355813)
- 624 Wei, H.-Z., Jiang, S.-Y., Hemming, N. G., Yang, J.-H., Yang, T., Wu, H.-P., Yang, T.-L., Yan,
625 X., & Pu, W. (2014). An improved procedure for separation/purification of boron from
626 complex matrices and high-precision measurement of boron isotopes by positive thermal
627 ionization and multicollector inductively coupled plasma mass spectrometry. *Talanta*,
628 123, 151-160. <https://doi.org/10.1016/j.talanta.2014.02.009>
- 629 Wei, H.-Z., Lei, F., Jiang, S.-Y., Lu, H.-Y., Xiao, Y.-K., Zhang, H.-Z., & Sun, X.-F. (2015).
630 Implication of Boron Isotope Geochemistry for the Pedogenic Environments in Loess and
631 Paleosol Sequences of Central China. *Quaternary Research*, 83(1), 243-255.
632 <https://doi.org/10.1016/j.yqres.2014.09.004>
- 633 Zeebe, R. E., & Rae, J. W. B. (2020). Equilibria, kinetics, and boron isotope partitioning in the
634 aqueous boric acid–hydrofluoric acid system. *Chemical Geology*, 550, 119693.
635 <https://doi.org/10.1016/j.chemgeo.2020.119693>
- 636